Protein Modifications Affecting Triplet Energy Transfer in Bacterial Photosynthetic Reaction Centers

Philip D. Laible,*# Veeradej Chynwat,§ Marion C. Thurnauer,# Marianne Schiffer,* Deborah K. Hanson,* and Harry A. Frank§

*Center for Mechanistic Biology and Biotechnology and #Chemistry Division, Argonne National Laboratory, Argonne, Illinois 60439, and §Department of Chemistry, University of Connecticut, Storrs, Connecticut 06269 USA

ABSTRACT The efficiency of triplet energy transfer from the special pair (P) to the carotenoid (C) in photosynthetic reaction centers (RCs) from a large family of mutant strains has been investigated. The mutants carry substitutions at positions L181 and/or M208 near chlorophyll-based cofactors on the inactive and active sides of the complex, respectively. Light-modulated electron paramagnetic resonance at 10 K, where triplet energy transfer is thermally prohibited, reveals that the mutations do not perturb the electronic distribution of P. At temperatures $\geq$ 70 K, we observe reduced signals from the carotenoid in most of the RCs with L181 substitutions. In particular, triplet transfer efficiency is reduced in all RCs in which a lysine at L181 donates a sixth ligand to the monomeric bacteriochlorophyll B_B. Replacement of the native Tyr at M208 on the active side of the complex with several polar residues increased transfer efficiency. The difference in the efficiencies of transfer in the RCs demonstrates the ability of the protein environment to influence the electronic overlap of the chromophores and thus the thermal barrier for triplet energy transfer.

INTRODUCTION

In the first steps in the conversion of light energy to chemical energy, primary charge separation occurs in a transmembrane pigment-protein complex known as the photosynthetic reaction center (RC). The RC of purple nonsulfur bacteria consists of three transmembrane subunits (L, M, and H) and several prosthetic groups; the complex is localized in unique invaginations of the intercytoplasmic membrane of these organisms. Electron transfer is initiated on a dimer of bacteriochlorophyll known as the special pair (P). After the arrival of an excited state from the light-harvesting antennae, electron migration proceeds from the primary donor P to a nearby bacteriopheophytin molecule (H_A) in ~3 ps. Subsequently the electron is transferred to the primary quinone (Q_A; in 200 ps), and finally to the terminal acceptor, the secondary quinone (Q_B; in 5–200 μs). As this process repeats, a proton gradient builds across the membrane, which is used to drive ATP synthesis. Once Q_B has acquired two electrons and two protons, the quinol diffuses from the complex to be replaced by another quinone from a large pool within the membrane.

When the organism is subjected to high-light conditions in nature, electron transfer to Q_A becomes blocked as the rate of conversion of light into charge-separated states in the RC exceeds the capacity of the soluble carriers involved in cyclic electron transfer. In that event, a well-characterized T_0-polarized triplet state ^TP is formed on P from $P^+H_A^-$ (Fig. 1; reviewed in Thurnauer, 1979). This unique polarization is due to the quantum mechanical mixing of the singlet and triplet states from which it arises. In a semiaerobic environment, the major role of the carotenoid (C), also bound by the RC, is to quench ^TP before its sensitization of the $^1\Delta_g$ singlet state of oxygen—a potentially damaging biological oxidant. The carotenoid performs this function in most bacterial RCs by rapidly accepting the triplet state from P and dissipating this excited state energy into heat through internal conversion. The lowest lying triplet states of the special pair and carotenoid are such that ^TP can promote oxygen to its excited singlet, whereas ^{T}

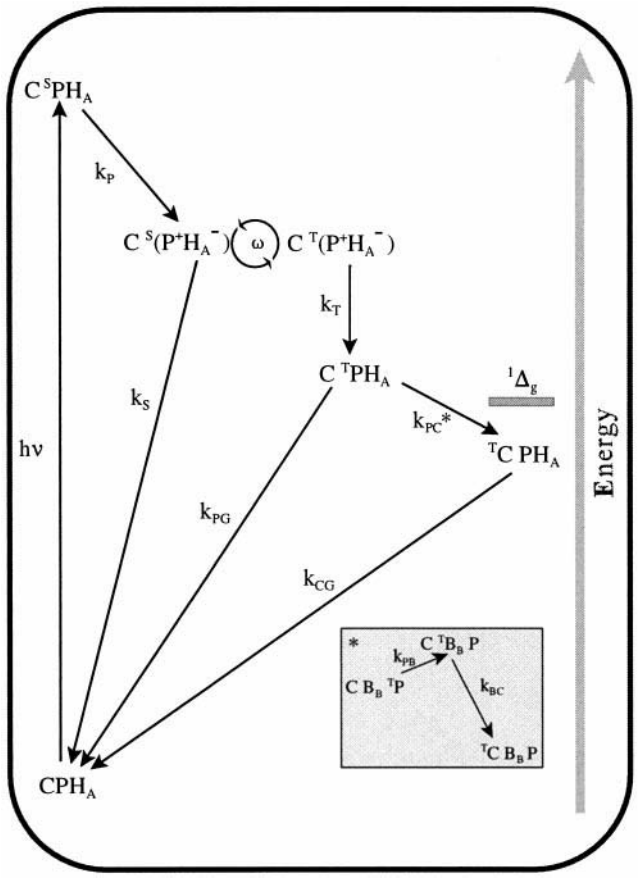

FIGURE 1 Summary of the relative energy levels of states and rate constants involved in light absorption, excited state energy transfer, and electron transfer (both forward and reverse (charge recombination)) in wild-type photosynthetic bacterial RCs with Q_A reduced by the addition of dithionite. Singlet and triplet excited-state species are denoted by superscripts S and T preceding the cofactors. Values for the rate constants were extracted from the literature on wild-type or carotenoidless strains of *Rb. capsulatus* at low temperature ($\leq$15 K) where possible, but data from room temperature experiments with *Rb. sphaeroides* RCs were routinely substituted: k_P, $\sim$[3 ps]$^{-1}$ (Kirmaier and Holten, 1987); k_S, [10–20 ns]$^{-1}$ (Schenck et al., 1982); k_Q, $\sim$[200 ps]$^{-1}$ (Kirmaier and Holten, 1987); ω, [30 ns]$^{-1}$ (Lang et al., 1990); k_T, $\sim$[2 ns]$^{-1}$ (Haberkorn et al., 1979; Norris et al., 1982; Kolaczkowski et al., 1990); k_{PG}, [10 μs]$^{-1}$ (Cogdell and Frank, 1987); k_{PC}, [30 ns]$^{-1}$ (Frank et al., 1996; 298 K); k_{CG}, [7 μs]$^{-1}$ (Frank et al., 1996). The relative energy level of singlet molecular oxygen ($^1\Delta_g$) is shown for comparison. (*Inset*) Steps in the triplet energy transfer reaction $^TP \rightarrow {}^TC$, showing the involvement of ^TB_B as an intermediate. The sum of rate constants k_{PB} and k_{BC} equals k_{PC} in the main diagram.

1) and is thought to be bound in a 15–15′-cis configuration (Arnoux et al., 1989). The presence of the carotenoid is known to influence the absorption spectrum of B_B; in *Rb. sphaeroides* RCs, its Q_y transition at 4 K shifts from $\sim$800 nm in the carotenoidless R-26 strain to 812 nm in a carotenoid-containing strain (Breton, 1988).

The nature of the triplet energy transfer is presumably controlled by the exchange mechanism described by Dexter (1953), which requires near-orbital overlap between the donor and acceptor species. Because the distance between P and the carotenoid is too large (Table 1) to allow the orbital

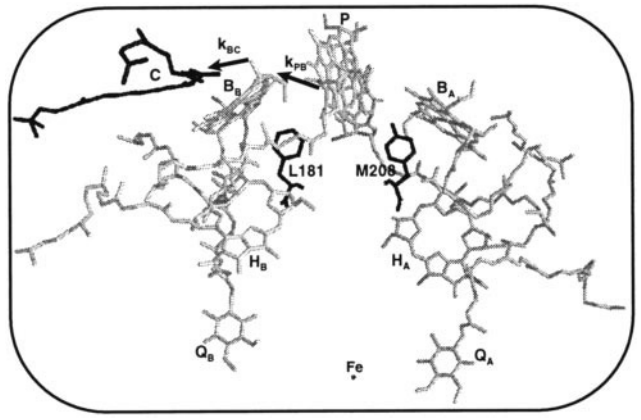

FIGURE 2 The structural positions of the substituted amino acids in relation to the cofactors, in particular, the dimer (P), monomers (B_A and B_B), and carotenoid (C) in the RC of purple nonsulfur photosynthetic bacteria (Ermler et al., 1994). Residues L181Phe and M208Tyr (M210 in *Rb. sphaeroides*) represent a conserved asymmetry that was targeted for mutation in this study. Sizable cavities introduced by the substitution of smaller residues in this hydrophobic region of the structure are likely to be filled by water molecules (Schiffer et al., 1995). The sum of rate constants k_{PB} and k_{BC} equals k_{PC} (Fig. 1).

overlap required for efficient exchange, the transfer must involve the bridging monomeric bacteriochlorophyll species, B_B. Recent work on RCs in which the native B_B was exchanged with other types of chlorophyll molecules, after which the native carotenoid was reconstituted (Frank et al., 1993a, 1996), has demonstrated this point. These optical and electron paramagnetic resonance (EPR) studies revealed that the yield of the ^TC signal at temperatures between 95 and 150 K is dependent upon the triplet energy level of the molecule bound at the B_B site and that the transfer process is thermally activated. However, in these experiments it was not clear whether B_B participated as an intermediate in a stepwise transfer or as a partner in a superexchange process. A monomeric triplet state has been observed by absorption-detected magnetic resonance (ADMR) techniques at low temperature in carotenoidless reaction centers from *Rhodobacter sphaeroides* (Angerhofer and Aust, 1993); although the triplet could form on B_A with a low yield as a result of recombination of the radical pair $^3[P^+H_A^-]$, the 812-nm ADMR bleaching is suggestive of localization on B_B (Hartwich et al., 1995).

The carotenoid is "protective," i.e., able to quench triplet states from the special pair, in RCs of *Rb. sphaeroides* and *Rb. capsulatus*, but not in RCs of *Rps. viridis*. The most

TABLE 1 Distances (Å) between cofactors in the RC structure (Ermler et al., 1994) involved in triplet energy transfer

Cofactors	Closest contact, Å	Center-to-center distance, Å
P and C	11.2	17.0
P and B_B	3.8	5.6
B_B and C	4.8	11.0
H_B and C	7.3	12.5

likely difference between these species was suggested by the work of Takiff and Boxer (1988a,b), who showed by phosphorescence spectroscopy that the energy gap between ^{T}P and $^{T}B_B$ is much larger in *Rps. viridis*, which contains bacteriochlorophyll *b*, than it is in *Rb. sphaeroides*, which contains bacteriochlorophyll *a*. A larger energy gap between the ^{T}P and $^{T}B_B$ states would inhibit the thermally activated triplet transfer. The electronic distribution of the P in *Rps. viridis* might also be influenced by small changes in the protein environment, or by the effects of the bound cytochrome. Mutations that alter the pigment composition of P or B_B in other species have also been shown to affect triplet transfer efficiency. In the bacteriochlorophyll-bacteriopheophytin "heterodimer" mutants of *Rb. capsulatus* and *Rb. sphaeroides* (Bylina et al., 1990; Frank et al., 1993b; respectively), light-modulation EPR results showed that triplet transfer was more efficient than in the wild-type RC. In the M180His → Arg mutant in *Rb. capsulatus*, the protein ligand to B_B was modified, and triplet energy transfer to the carotenoid does not occur at 6 K or 100 K.

The rate of triplet transfer in native RCs of *Rb. sphaeroides* has been directly measured using standard, time-resolved optical techniques by monitoring the rise of a triplet-triplet absorption of the carotenoid (Schenck et al., 1984; Frank et al., 1996). Those experiments showed a temperature dependence for the triplet transfer reaction; the rate ranged from $[250\ \text{ns}]^{-1}$ at 40–50 K to $[30\ \text{ns}]^{-1}$ at room temperature, with an activation barrier in the wild type of 140 cm^{-1}. In contrast, the EPR measurements of Hoff and Proskuryakov (1985) indicate substantially lower rates of ^{T}P decay (presumably representing triplet energy transfer to the carotenoid) of $[20\ \mu\text{s}]^{-1}$ and $[4\ \mu\text{s}]^{-1}$ at 40 K and 60 K, respectively.

The above studies demonstrated that the rates of triplet excited-state energy transfer are influenced by the triplet state energies, orbital overlaps, and electronic distributions of the three molecular species (P, B_B, and C) involved in the excited-state energy transfer. In the work presented here, we have evaluated the ability of the protein to influence the rate of triplet energy transfer in bacterial RCs by determining the energy transfer efficiency for the members of a large family of strains carrying site-specific substitutions for the symmetry-related residues L181Phe and M208Tyr (Fig. 2). These conserved residues are in proximity to B_B and/or P, and the substitutions in the mutants are known to affect the redox potential, rates of primary electron transfer, and 4 K absorption spectra of RCs (Jia et al., 1993; Popov, 1996; DiMagno et al., 1997).

We report results from light modulation EPR measurements and computer simulations which demonstrate that the efficiency of triplet energy transfer from the primary donor to the carotenoid in mutant RCs of *Rb. capsulatus* can vary widely. The results, which are interpreted using the RC structure (Fig. 2), show that changes in the protein can influence the electronic distribution and spatial overlap of the chromophores and/or adjust the thermal barrier for triplet energy transfer. Our results define more thoroughly the role of the bacteriochlorophyll monomer in bridging the transfer of triplet energy from the primary donor to the carotenoid.

MATERIALS AND METHODS

Construction and culture of mutant strains, and chromatophore isolation

The construction of site-specific mutations at the L181 or M208 sites has been described (DiMagno et al., 1997). To construct the L181-M208 double mutants, intermediate pU2922 derivatives (Bylina et al., 1989) were made that carried the L181 mutation coupled to a *Bgl*II-tagged version of the M gene, or alternatively, a *Bal*I-tagged L gene was coupled to the M208 mutation. Loss of the appropriate restriction site was used to indicate the switching of the corresponding mutant L- or M-gene for the tagged version. Mutant derivatives of pU2922 were transferred to *Rb. capsulatus* deletion strain U43 (Youvan et al., 1985; $LH1^-$, $LH2^-$, RC^-) via conjugation with *Escherichia coli* donor strain S17-1 (Simon et al., 1983); for the construction of carotenoidless strains, conjugations utilized *Rb. capsulatus* deletion strain U43B (Kolaczkowski et al., 1990). The carotenoid-containing "wild-type" strain [$LH1^+$, $LH2^-$, RC^+] is U43 complemented *in trans* by plasmid pU2922. The M208Tyr → Cys mutant was isolated as a photocompetent phenotypic revertant of the photosynthetically incompetent (PS^-) M208Arg strain.

All strains were grown under chemoheterotrophic conditions (semiaerobic, dark, 34°C) on RCVPY medium (Xiao et al., 1994) containing 30 μg/ml kanamycin. Membrane fragments (chromatophores) were prepared from solution cultures according to the method of Prince and Youvan (1987), with modifications described below. Briefly, cells were washed and sonicated in 10 mM Tris (pH 7.3) and subsequently disrupted with a French press. Chromatophores were recovered by ultracentrifugation at 4°C of lysate devoid of cell debris to which lauryldimethylamine oxide (LDAO) had been added to a final concentration of 0.05%. Chromatophore pellets were resuspended in small volumes of cold Tris buffer (pH 7.3) with a small paint brush and cold tissue homogenizer (Teflon piston/glass barrel unit) and diluted to an $OD_{875\ nm}$ of 35–60 (1-cm path; concentrations were routinely determined using 1:50 or 1:100 dilutions). Samples were stored at −70°C. Steady-state absorption spectra from 250 to 1000 nm were recorded with a Shimadzu Scientific Instruments spectrophotometer (model UV1601-PC).

Light-modulated EPR spectroscopy

EPR samples were prepared by mixing 300 μl of the sample with an $OD_{875\ nm}$ of ~50 (1-cm path) with 40 μl of degassed ethylene glycol and ~5 mg of sodium dithionite. The samples were then introduced into 3-mm inner-diameter EPR tubes that were sealed with septum caps, and kept under liquid nitrogen. EPR spectra were recorded with a Bruker ESP300 instrument equipped with an ER 023 M signal channel, an ESP1600 1070 10-MHz digitizer, an ER 032 M field controller, and an ER 041 MR bridge. Operating Systems version 9 (OS9/680) was used with 1 MB base memory. An Oxford ITC4 helium temperature controller and an ESR 900 cryostat were used to achieve temperatures of $\leq 70 \pm 0.5$ K. A Eurotherm B-VT 2000 nitrogen temperature controller was used for temperatures of 110 ± 0.5 K. A 1000-W xenon arc lamp was the light source. The light was filtered by 8 cm of water in a Pyrex bottle and passed through a light chopper of local design that modulated the light at 100 Hz. The modulated light was then focused into a ER 4102 STO standard rectangular cavity equipped with a 100% light-transmitting front flange for the light access. The DC output of the EPR magnetic field modulation amplifier (signal channel ER 023 M) was fed to an external lock-in amplifier (EG&G model 128A) referenced to the 100-Hz frequency of the modulated light source. The output from the external lock-in amplifier was then fed directly back to the digitizer and into the EPR computer system. The EPR conditions were as follows: microwave power, 20.5 mW; field modulation frequency,

100 kHz; field modulation amplitude, 5 G; receiver gain, 1×10^4 to 1×10^5; sweep time, 5.6 min; signal channel time constant, 0.16 s; digitizer time constant, 0.16 s; and light modulation lock-in time constant, 3 s. Spectra were the average of 2–16 scans. A modulation amplitude of 14.2 G and an average of 9–16 scans were used for samples with low concentration or low signal intensity. Microwave frequency for each sample in measurements made with the Oxford cryostat and the liquid nitrogen Dewar flask, was 9.380 ± 0.004 and 9.340 ± 0.004 GHz, respectively.

Data analysis and simulation

Computer simulations of the *Rb. capsulatus* triplet state EPR spectra (both ^{T}P and ^{T}C) were performed by methods reported previously by Frank et al. (1979) and further refined by McGann and Frank (1985 and references therein). Briefly, matrix solution techniques were applied to the system of differential equations describing the dynamics of an excited triplet state (comprising a vector **N** of time-dependent populations with three triplet sublevels N_i (where $i = -1$, 0, and $+1$)). The dynamics involve rate constants for triplet level population, depopulation, spin-lattice relaxation (T_1 processes), and radiative transitions (P_μ) in the high field limit:

$$\frac{d\mathbf{N}}{dt} = -\mathbf{kN} + \mathbf{A} \tag{1}$$

where **A** is a vector of populating rate constants A_i (i.e., initial triplet level distributions for each triplet sublevel, i) and **k** is a matrix of populating and depopulating (intersystem crossing) processes,

$$\mathbf{k} = \begin{bmatrix} -(k_{+1} + W_1 + W_2 + P_\mu) & W_1 + P_\mu & W_2 \\ W_1 + P_\mu & -[k_0 + 2(W_1 + W_2)] & W_1 + P_\mu \\ W_2 & W_1 + P_\mu & -(k_{-1} + W_1 + W_2 + P_\mu) \end{bmatrix} \tag{2}$$

In the matrix **k**, W_i are rate constants for spin-lattice relaxation, and k_i are rate constants for intersystem crossing that depopulates from the triplet sublevels to the ground state singlet. Because ^{T}P in bacterial photosynthetic RCs is spin-polarized by the radical pair mechanism (Thurnauer et al., 1975; Levanon and Norris, 1978) and ^{T}C is derived from ^{T}P, these triplet states are selectively populated in the T_0 sublevel. Thus the populating rate constant A_0 is nonzero, and A_{+1} and A_{-1} can be taken to be zero. EPR spectra were calculated by diagonalization of the appropriate Hamiltonian and the weighting of the intensities of the transitions by the difference in population between any two sublevels of the triplet state computed from Eq. 1. The method incorporates ensemble averaging of the EPR intensity over all possible orientations of the triplet principal magnetic axes with respect to the applied (Zeeman) field. Spectra were calculated on a Silicon Graphics Indigo computer. The output was compared directly to the experimental spectrum. Input parameters were modified until a qualitative agreement was reached between simulated and experimental spectra in the absence of a least-squares routine to optimize quantitatively the simulation inputs. Simulations were conducted only for pure ^{T}P (to mimic spectra from RCs in all strains at 10 K, or in carotenoidless strains at all temperatures) or pure ^{T}C (to mimic spectra from RCs of most strains at 110 K; see Discussion). Those spectra displaying both triplet lineshapes were produced by summing the best fit, computer-generated versions of the individual components. The relative proportions of the two components used in the combined spectrum were determined by the width of the observed features, the intensity of the respective signals at characteristic field positions, and the general qualitative agreement with the measured spectrum across the entire field sweep. The ratios of ^{T}P:^{T}C intensities were rounded to the nearest tenth. In simulations of data having reduced signal to noise, the median of a range of ^{T}P:^{T}C ratios that fit the experimental spectrum was selected.

As will be discussed below, the ratios of ^{T}P:^{T}C extracted from the 70 K and 110 K spectra represent the yields of the two known processes (triplet energy transfer, k_{PC}, and return to the ground state via intersystem crossing, k_{PG}; Fig. 1), which compete for deactivating the excited-state triplet energy on P. At temperatures where $k_{PC} \gg k_{CG}$ (Fig. 1), simple expressions relate the yields (Φ_{PG} and Φ_{PC}, respectively) of these processes to their rate constants:

$$^{T}P \cong \Phi_{PG} = \frac{k_{PG}}{k_{PG} + k_{PC}} \tag{3}$$

$$^{T}C \cong \Phi_{PC} = \frac{k_{PC}}{k_{PG} + k_{PC}} \tag{4}$$

The exactness of the initial equalities in Eqs. 3 and 4 (relating the intensities of triplet features of the special pair ^{T}P and carotenoid ^{T}C observed in the light-modulated EPR spectra to the yields of energy transfer and relaxation processes) depends 1) on the relative magnitudes of k_{PG} and k_{CG} (Fig. 1), because a longer-lived spin-polarized state will contribute more significantly to the steady-state nature of light-modulated EPR spectra, and 2) on the relative integrated area of the triplet signals from ^{T}P and ^{T}C, which we assume to be equal in this study. Because ^{T}C is known to decay more rapidly (especially at low temperature; Cogdell and Frank, 1987; Frank et al., 1996), signals originating from the carotenoid are inherently less intense than are signals originating from ^{T}P.

RESULTS AND DISCUSSION

Summary of mutant strains

The RCs in this study carry site-specific mutations of residues L181Phe and/or M208Tyr. The positions of these residues in relation to the cofactors in the wild-type *Rb. sphaeroides* RC structure (Ermler et al., 1994) are shown in Fig. 2. Although the L181Phe-M208Tyr asymmetry is conserved in several species of photosynthetic bacteria, the hydroxyl group of M208Tyr does not form a hydrogen bond with any of the cofactors of the active branch of the RC. L181Phe and M208Tyr are approximately equidistant from four cofactors—both bacteriochlorophyll molecules of the dimer, and the monomeric bacteriochlorophyll and bacteriopheophytin molecules of their respective cofactor branches. These contacts for a tyrosine at position L181 would be similar to those of M208Tyr on the opposite branch, with the exception that the distances would be 0.3–0.5 Å greater (DiMagno et al., 1997). Residues M208 and L181 are located in an extremely hydrophobic region of the RC; therefore it is not expected that any of the acidic or basic residues that have been substituted at L181 or M208 will be ionized. It is expected that any substantial cavities that are introduced by the substitution of smaller residues will be filled by water molecules (Schiffer et al., 1995). Table 2 includes a complete description of the strains used in this study; it includes known and potential effects of the substitutions and our rationale for including particular strains to aid in the interpretation of the data.

Description of magnetic axes of ^{T}P and ^{T}C

Two spin-polarized triplets, ^{T}P and ^{T}C, have been observed and characterized in bacterial RCs. The L181/M208 mutant

TABLE 2 Mutant strains used in this study with a summary of triplet features observed at 10, 70, and 110 K, using light-modulated EPR techniques

Strain name	Protein sequence	Known effects of mutation(s)*	10 K features			Ratios of $^{T}P:^{T}C$			Transfer class
			$\|D\|$, cm^{-1}	$\|E\|$, cm^{-1}[#]	$P_Z:P_X$[§]	10 K	70 K[¶]	110 K[¶]	
FE	L181Phe M208Glu	Acidic residue on A-side	0.0186	0.0033	2.0	∞	0.6	0.0[‖]	I
FC	L181Phe M208Cys	Polar residue on A-side	0.0187	0.0032	1.4	∞	0.6	0.1	I
EE	L181Glu M208Glu	Acidic residues on A- and B-sides	0.0187	0.0033	1.7	∞	0.8	0.2	I
FH	L181Phe M208His	H-bond to H_A	0.0186	0.0031	2.6	∞	0.7	0.4	I
FT	L181Phe M208Thr	Small polar residue on A-side	0.0186	0.0033	1.7	∞	0.8	0.4	I
FA	L181Phe M208Ala	Potential cavity on A-side	0.0187	0.0032	2.0	∞	0.9	0.4	I
FK	L181Phe M208Lys	Basic residue on A-side	0.0186	0.0032	2.2	∞	0.8	0.5	II
WT (wild type)	(L181Phe M208Tyr)	Native carotenoid-containing *Rb. capsulatus*	0.0185	0.0030	2.0	∞	0.8	0.5	II
WT C^- (wild type)	(L181Phe M208Tyr)	Native carotenoidless *Rb. capsulatus*	0.0186	0.0030	2.0	∞	∞	∞	—
TT	L181Thr M208Thr	Small polar residues on A- and B-sides	0.0189	0.0034	1.4	∞	0.9	0.5	II
EY	L181Glu M208Tyr	Acidic residue on B-side	0.0186	0.0031	2.0	∞	0.9	0.5	II
HH	L181His M208His	H-bonds to H_A and H_B	0.0185	0.0030	2.1	∞	1.0	0.5	II
FF	L181Phe M208Phe	Phe symmetry on A- and B-sides	0.0186	0.0031	2.4	∞	1.0	0.6	II
TY	L181Thr M208Tyr	Small polar residue on B-side	0.0185	0.0031	2.2	∞	1.2	0.5	II
TTP	L181Thr M208Thr M271Pro	Phenotypic revertant (PS^+) of TT (PS^-)	0.0189	0.0034	1.5	∞	1.3	0.5	II
HY	L181His M208Tyr	H-bond to H_B	0.0186	0.0031	2.2	∞	1.3	0.6	III
AY	L181Ala M208Tyr	Potential cavity on B-side	0.0186	0.0032	2.0	∞	1.5	0.7	III
YY	L181Tyr M208Tyr	Tyrosine symmetry on A- and B-sides	0.0186	0.0031	1.9	∞	1.6	0.7	III
KE	L181Lys M208Glu	Acidic residue on A-side; hexacoordinated B_B	0.0186	0.0032	1.5	∞	1.7	0.7	III
KK	L181Lys M208Lys	Basic residue on A-side; hexacoordinated B_B	0.0186	0.0032	1.8	∞	1.8	0.9	III
KY	L181Lys M208Tyr	Hexacoordinated B_B	0.0185	0.0032	2.0	∞	1.8	1.0	III
KY C^-	L181Lys M208Tyr	Hexacoordinated B_B in carotenoidless background	0.0187	0.0032	1.3	∞	∞	∞	—
YF	L181Tyr M208Phe	Reversal of wild-type sequence	0.0186	0.0031	2.9	∞	2.6	1.0	III

*Because of the hydrophobic environment, we do not expect the acidic or basic residues at L181 and M208 to be ionized, but they would carry partial charges.

[#]Average of the zero-field-splitting parameter E from the field spacing of the X ($D + 3E$) and Y ($D - 3E$) absorption and emission features of P.

[§]The ratio of relative intensities of the $|P_Z|$ and $|P_X|$ triplet features of the special pair in the spectra of the wild-type and mutant strains at 10 K. The reported values are averages of absorptive $|P_{Z(a)}:P_{X(a)}|$ and emissive $|P_{Z(e)}:P_{X(e)}|$ ratios.

[¶]Computer simulations were used to extract the contribution of ^{T}P and ^{T}C to the experimentally observed spectra at 70 K and 110 K.

[‖]This ratio has been defined as 0.0, although it may be up to 5% ^{T}P.

substitutions are positioned within the structure of the RC so that they can readily influence the electronic distribution and magnetic axes of the special pair, but are quite distant from the electronic cloud of the carotenoid and its magnetic axes. The magnetic properties of these triplets are described below.

Special pair

From work involving magnetophotoselection or the rotation of single RC crystals within a magnetic field, triplet studies have presented a model for the principal magnetic axes of the special pair relative to the molecular structure of the dimer (Norris et al., 1989; and reviewed in Budil and Thurnauer, 1991). In the *Rb. sphaeroides* R-26 RC, where the triplet is symmetrically shared on the L and M halves of the dimer, the z axis is orthogonal to the plane defined by the macrocycles of the bacteriochlorophyll molecules. The y and x axes are perpendicular to the z axis and point in the direction of the membrane and membrane normal, respectively. The y magnetic axis is aligned with the Q_y transition of P at 870 nm (Thurnauer and Norris, 1976; Frank et al., 1979).

Carotenoid

Although relatively less scrutinized, two prominent magnetic axes (the C_X and C_Y components, which have relatively slow depopulation rates) of the carotenoid have been suggested to lie along the linear halves of the *cis*-oriented carotenoid (McGann and Frank, 1985; Frick et al., 1990). The z axis thus lies orthogonal to both the C_X and C_Y projections and the plane of the carotenoid, pointing in the direction of the membrane normal.

Influence of mutation on ^{T}P

Spectra at 10 K

In triplet spectra, the zero-field splitting parameter $|D|$ reports the average distance between the two unpaired electrons, and parameter $|E|$ reflects the deviation of the triplet state spin system away from axial symmetry as well as the extent of π-delocalization. The values of $|D|$ and $|E|$ in the light-modulated triplet spectra observed at 10 K in the wild-type and mutant strains used in this study are summarized in Table 2. Representative spectra are shown in Fig. 3. Assignments of spectral features of ^{T}P follow the conventions of Budil and Thurnauer (1991) and Chadwick and Frank (1986); the absorptive (a) and emissive (e) signals are denoted in Fig. 3. The zero-field-splitting values of the aee-aae polarized triplets observed at this temperature indicate that the photoinduced excited electronic state is entirely localized on P in most (if not all) of the samples; thus triplet energy transfer to the carotenoid at 10 K is thermally prohibited in all RCs studied. Thus the ambient energy ($kT \approx 6.9$ cm^{-1} at 10 K, where k is the Boltzmann constant and T is the temperature in degrees Kelvin) is much lower than the barrier for the activated triplet energy transfer to the carotenoid.

The zero-field-splitting values ($|D| = 0.0185$ cm^{-1}; $|E| = 0.0030$ cm^{-1}) reported here for the wild-type *Rb. capsulatus* RCs are similar to those previously reported for membrane-bound *Rb. capsulatus* RCs (Bylina et al., 1990; Prince and Youvan, 1987). However, those authors had noticed a small

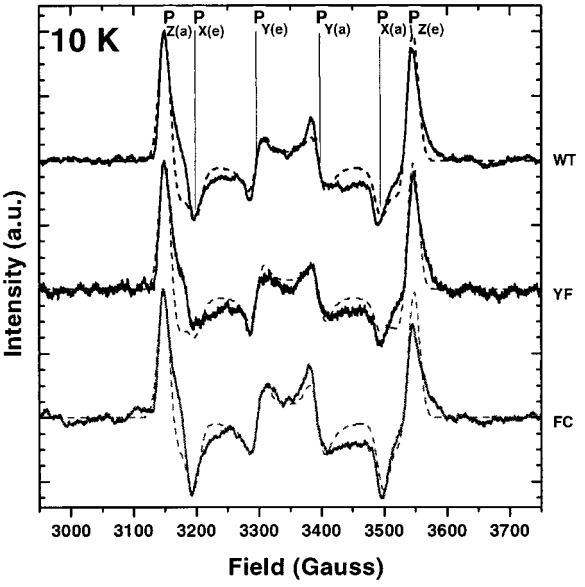

FIGURE 3 Representative light-modulated (——) and simulated (– – –) triplet EPR spectra of membrane-bound wild-type and mutant RCs with Q_A reduced by dithionite at 10 K. The spectra displaced about their zero baselines are offset for clarity and comparison. The substitutions carried by the mutant strains are summarized in Table 2. The convention adopted for the assignment of *X*, *Y*, and *Z* triplet spectral features (where a stands for absorptive and e stands for emissive) for ^{T}P is that of Budil and Thurnauer (1991), Chadwick and Frank (1986), and Bylina et al. (1990). The zero-field splitting parameters for the wild-type and mutant simulations are as reported in Table 2. The relative zero-field depopulating rate constants (k_X:k_Y:k_Z) that varied with RC mutation are 7:7:1 for WT; 12:7:1 for YF; and 4.2:5:1 for FC. Additional simulation parameters that were held constant in all strains at 10 K were as follows: relative populating rate constants (A_{+1}:A_0:A_{-1}), 0.0:1.0:0.0; intrinsic linewidth parameters, 13.2 G; $W_1 = W_2 = 0$. The microwave frequency for each sample was 9.380 ± 0.004 GHz.

difference (≤5%) in $|D|$ and $|E|$ values between membrane-bound and detergent-isolated *Rb. capsulatus* RCs with the triplet more localized in detergent-isolated systems. These differences may reflect small structural changes that are introduced by the interaction of the RC with the core LH1 antenna in membrane-bound systems.

The similarities in the positions of the triplet features in the spectra ($|D| = 0.0185$–0.0189 cm^{-1}; $|E| = 0.0030$–0.0034 cm^{-1}) indicate that the substitutions at L181 and M208 induce few effects on zero-field-splitting parameters of P. This suggests that the electronic distribution of the primary electron donor is not significantly perturbed in these mutant strains. Using simple orbital models (reviewed in Budil and Thurnauer, 1991), it can be shown theoretically that $|D|$ is inversely related to the average distance between the delocalized electrons of the triplet state. The small (<2%) change in $|D|$ that we observed with the substitutions at L181 and M208 reflects changes in the delocalized electronic distribution of P.

We note a change in the relative amplitudes of P_Z, P_X, and P_Y (Fig. 3) with mutation. These changes are likely to be associated with perturbations in the relative rates of

decay to the ground state via intersystem crossing from the *Z*, *X*, and *Y* triplet levels of P. Simulations in which the relative *X*, *Y* and *Z* intersystem crossing rates are varied reproduce the 10 K mutant spectra well, as shown by the fits to the spectra in Fig. 3. The caption to Fig. 3 summarizes the changes of the wild-type parameters that were required to reproduce the mutant spectra, in addition to the small changes noted in the zero-field-splitting parameters (Table 2). $|D|$ and $|E|$ are most perturbed in the RCs of TT and TTP; the relative intersystem crossing times from P_X are longest in the RCs of the TT, TTP, FC, EE, FT, and KE mutants and are shortest in RCs of the FF, FH, and YF mutants. These changes are reproducible and indicate variation in the electronic environment of P.

Asymmetry in spectral features

At 10 K, spin-lattice relaxation (SLR, or energy transfer between triplet sublevels; represented by W_1 and W_2 in Eq. 2) is not expected to be a dominant process influencing the ^{T}P spectra; if present, it could be observed with low-frequency light-modulation techniques (Norris and Thurnauer, 1978). In the absence of SLR, one would expect identical intensities of absorption and emission lines in symmetry-related positions on the opposite sides of $g = 2$, producing highly symmetrical triplet spectra, in contrast to the asymmetry that we have observed (e.g., Fig. 3). The increased amplitudes of the absorption lines (and decreased amplitudes of emission lines) at high field suggest that SLR might be a contributing factor for the shape of the time-resolved triplet spectra at 10 K. Although there may be some influence of SLR on the spectra, the dominant contributions to the asymmetrical triplet spectra at 10 K are the limiting values of the time constants on the lock-in amplifier and signal channel of the EPR. When choosing the conditions for the field sweeps, our goal was to minimize any experimental artifacts while maximizing the signal-to-noise ratios. We could never completely eliminate the former to achieve an acceptable degree of the latter in all mutant strains. The effects of this electronic filtering can be most readily discerned by comparing experimental and simulated features at 10 K (Fig. 3). The direction of the scan (from low to high field) is apparent. In the end, all of the spectra presented in this study were acquired with conditions that were precisely the same at a given temperature; consequently, they can be compared directly with each other. In that sense, the spectra are consistent although slightly perturbed by the selected time constants for the data acquisition.

^{T}P at 70 K and 110 K

Triplet spectra from membrane-bound *Rb. capsulatus* RCs at temperatures above 40 K are mixtures of ^{T}P and ^{T}C as k_{PC} begins to compete effectively with k_{PG}. Our ability to monitor triplet energy transfer between these cofactors is dependent on how well we can determine the relative contribution of each species to the spectra at different temperatures. Unique field transitions for ^{T}P and ^{T}C in the broad spectrum (from 2900 to 2700 G) aid in this dissection; however, many of the strong triplet features of ^{T}P and ^{T}C overlap (e.g., P_Z and C_X), making relative quantification difficult. Simulations (and linear combinations thereof) are important tools by which we can accurately quantify the relative contributions of ^{T}P and ^{T}C in composite spectra. To increase the precision of the analysis, knowledge of the temperature dependencies of the spectra of the individual components is needed.

As a control, we investigated the temperature dependence of ^{T}P, using carotenoidless strains of *Rb. capsulatus* (Kolaczkowski et al., 1990). As expected, the triplet spectra showed ^{T}P signatures at all temperatures studied (data not shown). The 10 K spectrum of the carotenoid-containing RCs was identical to that of carotenoidless RCs. Although the zero-field-splitting values in the spectra from the carotenoidless RCs did not change with temperature, the relative intensities of the P_Z, P_X, and P_Y features did change at higher temperature. At 70 K and 110 K, the magnitude of P_X and P_Y increased ~50% relative to that of P_Z in both carotenoidless wild-type and mutant RCs (Table 3). We can account for these changes by invoking a temperature dependence in the relative rates of intersystem crossing or the introduction of spin-lattice relaxation at higher temperatures. Because the latter has been required for interpretation of ^{T}P signatures at elevated temperatures (Hoff and Proskuryakov, 1985), we introduced SLR into the simulations and kept the relative intersystem crossing rates constant at all temperatures. The quantity of SLR (both W_1 and W_2; Eq. 2) that we incorporated to simulate the experimental spectra was equal to three times k_Z (and thus 43% of k_X and k_Y) in the wild-type RC. This level of SLR allowed simulations to match experiment at higher temperatures in both the wild-type and mutant carotenoidless RCs, and was used in linear combinations of triplet simulations for carotenoid-containing RCs at higher temperatures (as discussed below). The amount of SLR needed at higher temperatures was assumed to be equal for all RCs studied.

The temperature dependence of the carotenoid signals is less understood and cannot be studied in the absence of ^{T}P, because this state is its precursor. Thus we must assume that ^{T}C spectra determined at 110 K resemble the carotenoid component present in mixed spectra at lower temperatures. The only changes we observe in the carotenoid spectra at

TABLE 3 Temperature dependence of the ratio of special pair triplet features in the wild type and the L181Lys (KY) mutant

	Average $\lvert P_X{:}P_Z \rvert$			
	Wild type		L181Lys (KY)	
Temperature (K)	C^+	C^-	C^+	C^-
10 K	2.0	2.2	2.0	1.4
70 K	1.1	1.6	1.1	1.1
110 K	2.0	1.6	1.4	1.1

elevated temperatures (140 K) are differences in the relative amplitudes of the *Z*, *X*, and *Y* features.

Although monomeric bacteriochlorophyll (Bchl) or bacteriopheophytin (Bpheo) triplet states in the RC have never been observed with EPR techniques, their contribution to our spectra at this signal-to-noise level cannot be completely ruled out. Monomeric Bchl and Bpheo triplet states formed via the spin-orbit coupled intersystem crossing have been studied extensively in vitro (for a review see Budil and Thurnauer, 1991). To estimate the position and sign of the monomeric triplet features in vivo, the zero-field-splitting parameters in vitro can be assumed. The polarization pattern would be that of the T_0-polarized B_B or H_B triplet accepted from ^TP. The *Z* features of the in vivo monomeric triplets would either overlap C_Z or appear between C_Z and P_Z in our spectra (zero-field-splitting $|D|$ values of 0.023 cm^{-1} and 0.026 cm^{-1} for Bchl *a* and Bpheo *a*, respectively; Thurnauer, 1979). The *Z* features of B_B would be expected to add destructively to C_Z and constructively to P_Z. The position and sign of the *X* and *Y* features of the monomeric triplets would be even more difficult to discern (with zero-field-splitting *E* values of 0.006 cm^{-1} and 0.004 cm^{-1} for Bchl *a* and Bpheo *a*, respectively; Thurnauer, 1979). However, the *Y* feature is dominant in the Bchl *a* triplet in vitro, suggesting that there may be potential for its resolution in the future. Detection of these states will rely heavily upon input from recent model systems in which triplet states are formed via mechanisms similar to those that occur in the RC (e.g., Krasnovsky et al., 1997). The present analysis assumes that the spectra observed at temperatures above 10 K are mixtures of ^TP and ^TC only.

Influence of mutation on triplet energy transfer from P to C

110 K data

Unlike the signals observed at 10 K, the spectra at 110 K (Fig. 4) show signals originating primarily from the carotenoid. Wild-type *Rhodobacter* RCs readily transfer triplet states formed on P to the carotenoid at temperatures above 100 K (Bylina et al., 1990; Frank et al., 1993a, 1996). Thus light-modulated EPR spectra from these species at temperatures above 100 K are dominated by carotenoid signals. The carotenoid triplet is evident by its larger zero-field-splitting values and the opposite sign of *D* (producing ^TC spectra with an eaa-eea polarization pattern versus the aee-aae pattern of ^TP). From linear combinations of ^TP and ^TC simulations, we have deduced that ^TP contributes 33% (^TP:^TC ratio of 0.5; Table 2) to the signal observed at 110 K in the wild-type spectrum, indicating that triplet energy transfer to the carotenoid is beginning to compete effectively with the decay of ^TP to the ground-state singlet via intersystem crossing (k_{PG}; Fig. 1). Thus ambient energy ($kT \approx 76.4$ cm^{-1} at 110 K) is approaching values that overcome the uphill k_{PB} step in triplet energy transfer for the wild-type RCs studied. However, this is not true for all of the strains, as several of the mutants display an increased proportion of features characteristic of ^TP, whereas others completely lack any ^TP contribution at 110 K (Fig. 4).

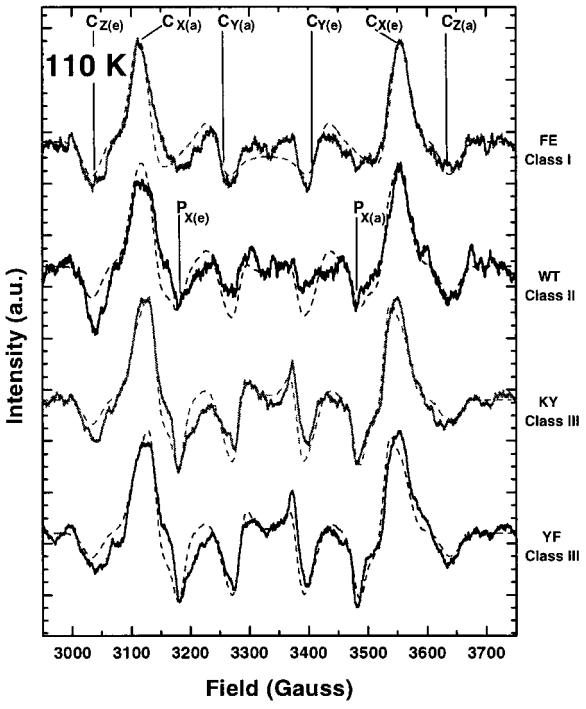

FIGURE 4 Representative light-modulated (——) and simulated (– – –) triplet EPR spectra of membrane-bound wild-type and mutant RCs with Q_A reduced by dithionite at 110 K. Mutant designations are as described in Table 2; the spectral assignments of *X*, *Y*, and *Z* triplet spectral features (where a stands for absorptive and e stands for emissive) for ^TP follows the convention adopted by Budil and Thurnauer (1991), Chadwick and Frank (1986), and Bylina et al. (1990). The *Rb. capsulatus* carotenoid triplet spectrum is defined as the 110 K spectrum of the FE mutant RC. The parameters used to simulate this carotenoid triplet are as follows: $|D| = 0.0282$ cm^{-1} and $|E| = 0.0042$ cm^{-1}; relative zero-field depopulating rate constants (k_X:k_Y:k_Z), 2.9:0.9:1.8; relative populating rate constants, (A_{+1}:A_0:A_{-1}), 0.0:1.0:0.0; intrinsic linewidth parameters, 21.5 G; no spin-lattice relaxation ($W_1 = W_2 = 0$). Although $|D|$ and $|E|$ zero-field-splitting parameters varied as reported in Table 2, only one set of parameters was used for all of the ^TP spectra used in the linear combinations at 70 K. The input parameters for that ^TP spectrum are as follows: relative zero-field depopulating rate constants (k_X:k_Y:k_Z), 7:7:1; relative populating rate constants (A_{+1}:A_0:A_{-1}), 0.0:1.0:0.0; intrinsic linewidth parameters, 13.2 G; relative rates of spin-lattice relaxation are three times k_Z or 43% of k_X and k_Y. The ratios of ^TP and ^TC needed to simulate the spectra are reported in Table 2. Note that at least one representative spectrum from each of the triplet transfer classes (vide infra) is included. The microwave frequency for each sample was 9.340 ± 0.004 GHz. The spectra displaced about their zero baselines are offset for clarity and comparison.

The ratios of ^TP:^TC needed to simulate the experimental spectra of all RCs are summarized in Table 2. The contribution of ^TP to the spectra at 110 K is most clearly seen as negative features at 3175 G ($P_{X(e)}$) and 3475 G ($P_{X(a)}$), and by the width of the strong positive transitions around 3125 G and 3550 G. Mutant RCs that appear to transfer most efficiently at 110 K include those with M208 mutations (Glu and Cys, and possibly His, Thr, and Ala substitutions). In particular, the spectra of the M208Glu (FE) and

M208Cys (FC) RCs demonstrate the complete absence of features associated at lower temperatures with ^{T}P. The similarity of signals from these two mutant RCs suggests that Cys, in combination with water molecules that fill the void caused by the substitution of this much smaller residue for Tyr, might result in an environment similar to that caused by the Glu substitution.

The 110 K spectrum of the FE mutant has been defined as the pure ^{T}C spectrum in this study. The simulated spectrum that accompanies the experimental plot for the FE mutant in Fig. 4 serves as the carotenoid component of the linear combinations in all RCs (including the wild type) at 70 K and 110 K.

It is apparent from the spectra in Fig. 4 and the ratios in Table 2 that many mutant RCs have reduced efficiencies of energy transfer compared to the wild type at 110 K. The most dramatically affected RCs are those with L181 mutations (in particular, the Lys substitution), and the YF strain, in which the conserved asymmetry in residues at positions L181 and M208 has been reversed. A more detailed discussion of the reduction in transfer efficiency follows the 70 K results.

70 K data

At 70 K, the native RC spectrum (Fig. 5) contains approximately equal contributions from the triplet states of the special pair and carotenoid (^{T}P:^{T}C = 0.8; Table 2). This implies that k_{PC} is approximately equal to k_{PG} (Fig. 1). Thus the ambient energy ($kT \approx 48.6$ cm^{-1} at 70 K) facilitates the slow uphill k_{PB} step in triplet energy transfer that can compete with k_{PG} at this temperature in the wild-type RCs. As seen in the above section, we observe reduced ^{T}C signals in RCs carrying substitutions at position L181 near B_B, and increased ^{T}C signals from many of the M208 mutants. As will be discussed below, the trends observed in the mutant RCs with reduced transfer efficiency at 70 K are also displayed at 110 K, with varied contributions of ^{T}P at 3190 G and 3490 G.

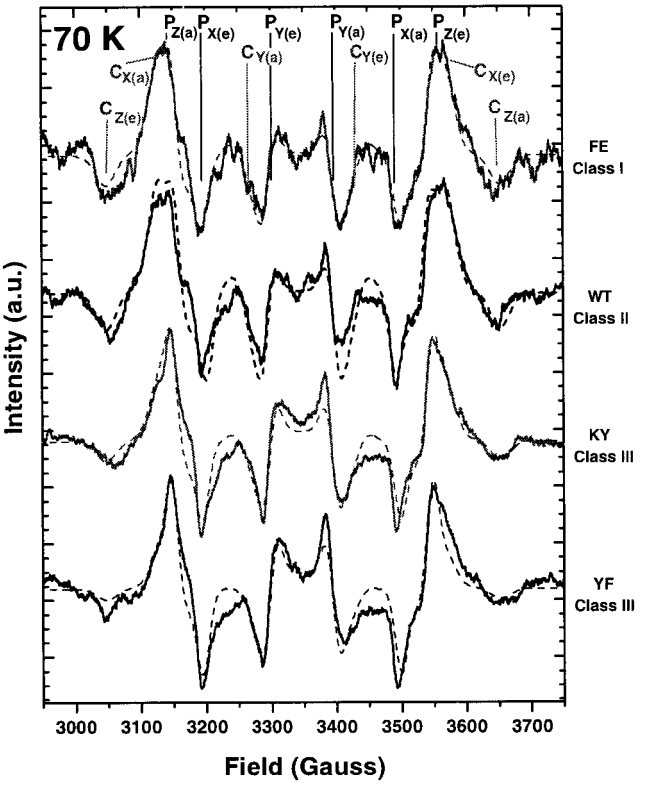

FIGURE 5 Representative light-modulated (——) and simulated (– – –) triplet EPR spectra of membrane-bound wild-type and mutant RCs with Q_A reduced by dithionite at 70 K. Spectral assignments, mutant descriptions, and ^{T}C and ^{T}P components of the simulated spectra are as in Fig. 4. The ratios of ^{T}P and ^{T}C needed to simulate the spectra are reported in Table 2. Note that at least one representative spectrum from each of the triplet transfer classes (vide infra) is included. The microwave frequency for each sample was 9.340 ± 0.004 GHz. The spectra displaced about their zero baselines are offset for clarity and comparison.

Mutant classes

We have classified the L181/M208 family of mutants into three categories based upon the 70 K and 110 K data. For reference, the mutant class assignments are identified in Table 2 and noted in Figs. 4 and 5. In addition, the ratios of ^{T}P:^{T}C at 70 K and 110 K are plotted together in Fig. 6 for all mutant RCs, which are listed in order of increasing ratio of ^{T}P:^{T}C at 110 K; mutant classes are noted on the figure. These assignments, based on the current data set, are subjective; additional data may show that there is little support for sharp distinctions between classes and that the data may be better described by a continuum.

Class I (more efficient than wild type)

Several mutants with substitutions at M208 [FE, EE, FC, FH, FT, and FA] show signs of increased triplet energy transfer efficiency relative to wild-type RCs. Class I mutants exhibit wild-type or slightly reduced ratios of ^{T}P:^{T}C at 70 K ($0.6 \leq {}^{T}\text{P}:{}^{T}\text{C} \leq 0.8$), but show significantly reduced ratios of ^{T}P:^{T}C at 110 K ($0.0 \leq {}^{T}\text{P}:{}^{T}\text{C} \leq 0.4$). In addition, FE may show some sign of a carotenoid signal at 10 K, although the signal-to-noise is not sufficient to make a conclusive statement (data not shown).

Class II (Wild type)

Many mutant RCs display an efficiency similar to that of wild-type RCs for transferring triplet energy from P to C. RCs in the wild-type class (FK, TY, EY, TT, TTP, FF, and HH) require relatively equal ($0.8 \leq {}^{T}\text{P}:{}^{T}\text{C} \leq 1.3$) contributions of simulated ^{T}P and ^{T}C components to describe the experimental spectra at 70 K. Triplet transfer to the carotenoid is possible at 110 K, but is only 60–70% efficient, based upon the amount of the ^{T}C component that is needed to simulate the experimental spectrum at this temperature (≈ 0.5 ^{T}P:^{T}C).

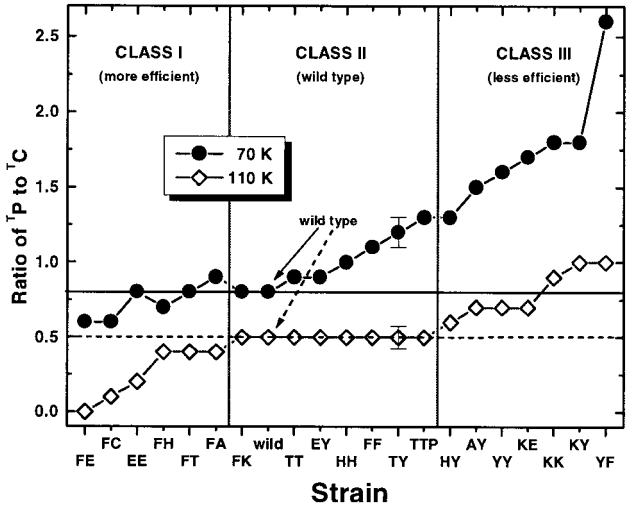

FIGURE 6 Ratio of ^{T}P:^{T}C needed in simulated spectra to mimic the experimental EPR spectra in wild-type and mutant strains at 70 K and 110 K. Mutants are arranged from left to right in order of increasing value of the ^{T}P:^{T}C ratio at 110 K. The error bars indicate the range of ratios of ^{T}P:^{T}C for which the linear combinations of simulations fell within the signal-to-noise ratio of the experimental spectra.

Class III (less efficient than wild type)

Several mutant RCs (HY, AY, YY, KE, KK, KY, and YF) show reduced efficiencies for triplet energy transfer and are grouped in a separate category. Spectra of these mutants show increased contributions of ^{T}P components at both 70 K ($1.3 \leq {}^{T}P{:}{}^{T}C \leq 2.6$) and 110 K ($0.6 \leq {}^{T}P{:}{}^{T}C \leq 1.0$). Every mutant RC in this class carries a substitution at L181, which may or may not be accompanied by an additional substitution at M208. The large decrease in the efficiency of transfer in the YF reaction center at 70 K suggests that this mutant RC (and similar ones yet to be identified) could possibly establish a fourth class.

Mechanisms by which substitutions could affect triplet energy transfer

At 70 K, wild-type *Rb. capsulatus* RCs exhibit positive (absorptive) signals from ^{T}P and ^{T}C at both low and high fields that are of equal amplitude ($|P_{Z(a)}{:}C_{X(a)}| \approx |P_{Z(e)}{:}C_{X(e)}| \approx 1$). This temperature is species-dependent; e.g., the comparable temperature in *Rb. sphaeroides* is 40 K (Frank et al., 1993a, 1996). Because the components in the energy transfer reaction are the same (P, B_B, and C), subtle changes in the protein environment must be involved in the tuning of the triplet energy levels or the orbital overlaps of the cofactors.

The differences in the temperature at which ^{T}P and ^{T}C appear at equal amplitude in the L181/M208 mutant RCs could be due to 1) variations in carotenoid binding and specificity; 2) changes in the intrinsic lifetime of ^{T}P; 3) a difference in the activation barrier for the reaction; and/or 4) structural changes of the protein and/or the cofactors that alter the coupling or electronic overlap between P, B_B, and C. We will examine each possibility separately and discuss evidence which suggests that one or a mixture of these effects can explain the current data set.

Carotenoid binding and specificity

Differences in carotenoid binding and/or specificity apparently do not contribute significantly to changes in the rates of energy transfer that we have observed. The $|D|$ and $|E|$ zero-field-splitting values of 0.0282 cm^{-1} and 0.0042 cm^{-1}, respectively, for carotenoid triplet are similar in the *Rb. capsulatus* wild-type and mutant RCs. They are also comparable to results obtained with detergent-isolated, spheroidene-reconstituted *Rb. sphaeroides* R-26 RCs (Chadwick and Frank, 1986), which displayed $|D|$ and $|E|$ values of 0.0286 ± 0.0006 cm^{-1} and 0.0044 ± 0.0003 cm^{-1}, respectively. These data suggest that spheroidene is the carotenoid that is bound in both wild-type and mutant *Rb. capsulatus* RCs. Spheroidenone is also in abundance within the chromatophores of *Rb. capsulatus*; however, spheroidenone-reconstituted *Rb. sphaeroides* RCs had distinctly different zero-field-splitting values ($|D| = 0.0271 \pm 0.005$ cm^{-1} and $|E| = 0.0042 \pm 0.0003$ cm^{-1}; Chadwick and Frank, 1986). Because the L181 and M208 mutations are sufficiently distant in the RC structures from the location of the functional group that differentiates spheroidene from spheroidenone (Ermler et al., 1994; Arnoux et al., 1995), these mutations are not likely to change the specificity of carotenoid binding in the mutant RCs. However, understanding of the carotenoid-protein interactions that specify binding is limited, because no specific interactions are evident between the polar group of the spheroidene and the protein residues in the crystal structure of *Rb. sphaeroides* 2.4.1 (Yeates et al., 1988). As these authors suggested, the data imply that interactions with bound detergent molecules, solvent, or membrane-spanning sections of the core LH1 antenna that have not yet been identified may be responsible for the carotenoid binding specificity.

Our data do not suggest that differences in ^{T}P:^{T}C ratios observed in the mutant strains are due to the incomplete occupancy of the carotenoid binding site. Scatter-corrected 4 K absorption spectra of several of the *Rb. capsulatus* mutant strains (DiMagno et al., 1997) reveal stronger absorptions between 19,250 cm^{-1} (520 nm) and 20,500 cm^{-1} (390 nm) at conserved energy positions relative to the carotenoidless *Rb. sphaeroides* R-26 strain. Although the integrated area of the broad, featureless carotenoid absorption in *Rb. capsulatus* RCs is difficult to quantify, the areas are qualitatively equal in spectra of wild-type and mutant RCs. In addition, binding in detergent-isolated RC preparations is fundamentally not quantifiable, as these spectra might not reflect (or would only represent the lower limit for) occupancies in membrane-bound RCs.

Influence on intrinsic lifetime of ^{T}P (effects on intersystem crossing rates)

Variability in the ^{T}P:^{T}C ratios may not only reflect changes in the rate of triplet transfer, but may also demonstrate the ability of the mutations to modify the intersystem crossing rate (or temperature dependence thereof) of the special pair from its spin-polarized triplet to the ground-state singlet (k_{PG}). Along these lines, spectra of RCs that look as though the rate constant for triplet transfer (k_{PC}) has been increased may just reflect an unchanged k_{PC}, but decreased k_{PG}. Likewise, spectra of RCs that look as though k_{PC} has been decreased may just reflect an increase in k_{PG}. The inability to separate these two effects with the light-modulation EPR data requires that both possibilities be entertained. (The two possibilities should be distinguishable by using Eqs. 3 and 4 and information obtained from the application of direct-detection, time-resolved EPR methods that monitor either the decay of ^{T}P or the rise of ^{T}C (both representing the sum of k_{PC} and k_{PG}) and yield estimates of the amount of ^{T}P that is converted to ^{T}C. These experiments are being conducted.)

Activation barrier

The data for several mutant RCs suggest that the activation barrier for triplet energy transfer is modulated by substitution of amino acids at the L181 and M208 positions. Energy transfer between P, B_B, and C can be related by

$$k_{PC} = k_{PB} + k_{BC} \quad (5)$$

Because $k_{PB} \ll k_{BC}$ in wild-type RCs, the slow step for triplet transfer to C from P is the step from P to B_B. In *Rb. sphaeroides*, the T_1 level of B_B is 140 cm^{-1} above that for P, making the triplet energy transfer extremely temperature dependent below 150 K when k_{PC} begins to compete with k_{PG}; the rapid $B_B \rightarrow C$ transfer step is downhill by 800-1200 cm^{-1} (Farhoosh et al., 1994; Frank et al., 1996). Applied to *Rb. capsulatus* RCs, these energy levels for the wild-type complex are depicted in Fig. 7 (*first column*). As compared to a temperature of 40 K for the *Rb. sphaeroides* RC, the results presented here show that the 1:1 ratio of ^{T}P:^{T}C occurs at 70 K in *Rb. capsulatus*. Using the Arrhenius expression,

$$k_{PC} = k_0 e^{(-E_a/kT)} \quad (6)$$

where E_a is the activation energy for the transfer and k_0 is k_{PC} at temperatures where $kT \gg E_a$, and assuming that the species require identical rates of triplet energy transfer to compete successfully with intersystem crossing of ^{T}P at the two temperatures, the data suggest that the activation barrier in *Rb. capsulatus* might be 7/4 higher than in *Rb. sphaeroides* (approaching 240–250 cm^{-1}).

The influences of the mutations on the activation barrier are reflected in the three right panels in the upper and lower rows of Fig. 7. The upper panel shows scenarios for the changes in the relative triplet levels that result in reduced rate constants for the transfer reaction (more efficient processes). Changes in the triplet levels of P and B_B can produce identical changes in E_a. Furthermore, both B_B and P could change in tandem in response to a particular mutation, which could yield an RC that has wild-type properties. Because $k_{PB} \ll k_{BC}$ (Eq. 5), the changes in the triplet energy of C will not significantly affect k_{PC}. The mutations are in proximity to both P and B_B and are distant from C.

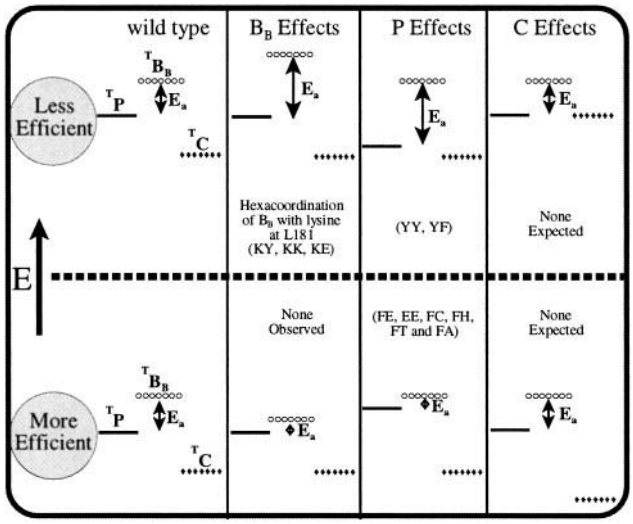

FIGURE 7 Potential changes in triplet energy levels of the three molecular species involved in energy transfer from the special pair to the carotenoid in bacterial photosynthetic RCs that could account for the observed increases and decreases in transfer efficiencies at various temperatures that are induced by mutations at positions L181 and M208 in the *Rb. capsulatus* RC. ——, ^{T}P; ○○○, $^{T}B_B$; ◆◆◆, ^{T}C.

Previous characterization of L181/M208 mutants helps explain the current data and assign the primary effects of the substitutions to a particular cofactor(s). As stated previously, the environment in this region of the RC is very hydrophobic; therefore we do not expect that acidic or basic residues will be ionized. It is expected that water molecules would fill sizable cavities that are generated by the substitution of much smaller residues for L181Phe or M208Tyr (e.g., Ala, Cys, Thr; Schiffer et al., 1995). Many slight mutation-induced changes are observed in the 4 K absorption spectra of purified RCs. The 4 K spectrum of the FK mutant RC indicates that the substitution of Lys for Phe at L181 provides a sixth ligand to B_B (Schiffer et al., 1992; DiMagno et al., 1997), yet there is no evidence for a similar effect on B_A when a lysine is substituted at M208 (P. D. Laible, M. Schiffer, and D. K. Hanson, unpublished observations). The effects of His substitutions at L181 and M208 are manifested as red shifts in the Q_x and Q_y transitions of the bacteriopheophytins; these shifts can be attributed to the formation of a hydrogen bond between the His and the ring I acetyl carbonyl atom of H_B or H_A (Schiffer et al., 1992; DiMagno et al., 1997). The rate of the $P^*H_A \rightarrow P^+H_A^-$ reaction is slowed by mutation of M208Tyr to Glu, Lys, Phe, and Thr (Jia et al., 1993; P. D. Laible and D. K. Hanson, unpublished observations). The rate of the $P^+H_A^-Q_A \rightarrow P^+H_AQ_A^-$ reaction is not significantly affected

by some mutations at M208 (e.g., Glu, Lys), but is slowed in RCs that carry a His substitution at M208 (P. D. Laible and D. K. Hanson, unpublished observations); these data are consistent with the effects of the His on H_A that are seen in the 4 K absorption spectrum. Redox titrations have shown that Thr, Phe, Lys, or His mutations at either M208 or L181 have equivalent effects on the midpoint potential of P; an exception is the Glu substitution at M208, which has a more substantial effect on the dimer redox potential than does the Glu mutation at L181 (Popov, 1996). From these data, we therefore expect that the primary effects of the L181/M208 substitutions, with the exception of His, will be manifested on P, B_A, and/or B_B.

Structural and environmental changes

Because the triplet energy transfer is dictated by the exchange mechanism of Dexter (1953) with an approximately exponential dependence on the edge-to-edge distance between cofactors (Lamola, 1969), we cannot rule out the influence that small structural perturbations of the protein and/or the cofactors will have on the electronic coupling between cofactors and thus the rate of this reaction. We invoke the experimentally verified description of triplet energy transfer via the Dexter mechanism as a two-electron transfer reaction with double the exponential distance dependence, 2β, of a single-electron transfer (Closs et al., 1989). β for a wide variety of electron transfer reactions in the RC has been shown generally to be 1.4 $Å^{-1}$ (as reviewed in Moser et al., 1992), which is the value that we will use in this analysis. Using distances presented in Table 1, we can quantify the effects of changes in the electronic overlap of cofactors on the rate of triplet transfer (assuming all other parameters—e.g., relative cofactor orientation, spectral overlap—are unchanged). In this analysis, a $\pm$1-Å change in the distance between P and B_B would result in a factor of $\mp$16 change in the rate constant for triplet transfer (where closer is faster). Therefore, small structural changes influencing the distance between and electronic overlap of P and B_B can perturb the reaction such that the energy transfer to C (k_{PC}) begins to compete with intersystem crossing to ground (k_{PG}) at a different temperature (Eqs. 3 and 4). The structural change that accompanies the hexacoordination of B_B upon substitution of a Lys for Phe at L181 might be sufficient to modify the rate by a structural rather than an activation barrier effect. The addition of this axial ligand should force B_B to adopt a more planar conformation (Callahan and Cotton, 1987), distorting the distance-dependent overlap of its electron orbitals with those of P. The distance between B_B and C is slightly larger (less critical; Table 1); however, a $\pm$1-Å change in their relative structural positions would result in changes in k_{BC} of a factor of $\mp$16—because of the nature of the distance dependence in exchange interactions (Dexter, 1953). Because the $B_B \rightarrow C$ step is not rate-limiting, this type of structural change would not contribute significantly to the overall k_{PC}.

Fig. 8 graphically depicts the effects that a particular mutation might exert on the return to the ground state via intersystem crossing of ^TP (k_{PG}), the activation barrier for k_{PC} (E_a), and/or the electronic coupling for the triplet energy transfer (an orbital overlap modification). Effects on any of these parameters will change the temperature dependence of the observed yield of triplet transfer, as monitored by the light-modulated EPR spectra. The expected temperature dependencies of k_{PG} and k_{PC} in wild-type *Rb. capsulatus* RCs are illustrated in solid gray and black lines, respectively. The yield of the process with rate k_{PC} is greater than that for k_{PG} above the "cross-over" temperature of 70 K, and is less than that for k_{PG} below 70 K in the wild-type RCs (Eqs. 3 and 4). The independent effects that a mutation could have on k_{PG}, E_a, or electronic coupling are shown in symbols; each of them would increase (in the cases shown) the cross-over temperature to 100^+ K from the wild-type 70 K, as observed with most Class III mutants. A line of solid squares represents potential mutational effects that increase k_{PG} at all temperatures; a line of open circles represents the potential mutational effects that increase E_a; and a line of asterisks represents the potential mutational effects that decrease the electronic coupling (through small changes in structure) involved in the triplet energy transfer reaction k_{PC}. The Arrhenius expression (Eq. 6) was used to construct these curves with appropriate parameter modification or with introduction of a scaling factor in the case of electronic coupling. With the current data set, the influences on k_{PG}, E_a, and electronic coupling are indistinguishable. This currently limits our ability to assign uniquely the consequences of the substitutions at positions L181 and M208. The interpretation is further complicated by the possibility that the mutations induce multiple effects that add or cancel deceivingly. Similar sets of curves can be constructed for the Class I mutants.

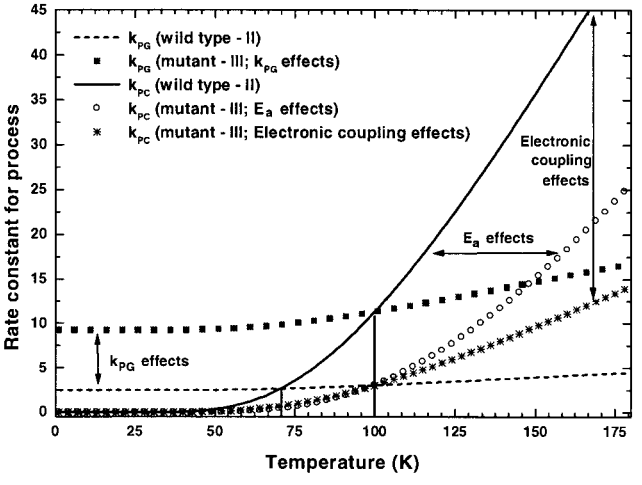

FIGURE 8 Temperature dependence of rate constants for triplet energy transfer k_{PC} and intersystem crossing from ^TP in wild-type bacterial RCs. Potential mutational effects on these rate constants that could explain the observed triplet signatures are shown for a visual depiction of statements in the text.

Insight into the mechanism of the P to C energy transfer

Because the mutations at L181 have a potential impact on k_{PC} by influencing B_B, the changes observed in k_{PC} with mutations at the symmetry-related M208 position might be occurring through regulation of the triplet energy level of B_A. Using known spacing for the triplet energy levels (Frank et al., 1996) and assuming that the triplet energy of $B_B = B_A$, we have calculated the Boltzmann population $p_i(B)$ of triplet energy on B_A, B_B, and P at various temperatures (Table 4) in both *Rb. sphaeroides* and *Rb. capsulatus*. In this calculation, the triplet state is partitioned between the three states involved ($N = 3$), based upon a maximum likelihood description of the system (see, e.g., Atkins, 1990), using the equation

$$p_i(B) = \frac{e^{(-E_i/kT)}}{\sum_{i=1}^{N} e^{(-E_i/kT)}}, \quad (7)$$

where E_i is the relative triplet energy of state i (B_A, B_B, or P). Of some surprise are the large (>20%) populations of B_A and B_B triplets at room temperature. Although at first glance they are less significant, the populations at temperatures between 70 K and 110 K are ≤12% on both monomers, and the triplet is completely localized on P at 10 K. An increase in triplet energy of 50 cm^{-1} for B_A in *Rb. capsulatus* changes the Boltzmann population on B_B (+0.2%), P (+3.1%), and B_A (−3.3%). Most of the redistribution of triplet populations occurs from B_A to P and not from B_A to B_B. Thus changes in the triplet energy of B_A cannot account for the observed changes in rates that we have observed with substitutions at M208. It is likely that M208 mutations affect k_{PC} solely by their influences on P. It is interesting to note that a 50 cm^{-1} decrease in the triplet energy level of B_A traps some of the excited-state energy on the A-side of the complex ($B_B = 6.0\%$, $P = 82\%$, and $B_A = 12\%$), but there are not substantial changes in the fraction residing on B_B. It is the large energy gap between the B_A/B_B and P that render the weighting relatively insensitive to small changes in the triplet energy levels of B_A and B_B.

The relative triplet energy levels of B_A and B_B are not known, and we have inferred here that their energy levels are identical, based upon their symmetrical placement around P. However, the singlet energy levels of B_A and B_B differ because the amino acids that surround them are not equivalent (El-Kabbani et al., 1991); thus the equivalence of ^TB_A and ^TB_B is questionable. The energy difference between the T_1 levels of P and B_B is known from the temperature dependence and pigment substitution work of Frank et al. (1993a, 1996). Because there is no carotenoid on the A-side, we cannot determine in a similar manner the energy difference between the triplet levels of P and B_A without additional input from other experiments. The triplet energy level of B_A might have an effect on k_{PC}, depending on the triplet energy difference between P and B_A.

TABLE 4 Temperature dependence of the Boltzmann populations of triplet occupation of the monomeric bacteriochlorophylls relative to the special pair in wild-type RCs from *Rb. sphaeroides* and *Rb. capsulatus*

Temperature, K (kT, cm^{-1})	*Rb. sphaeroides* (E_a = 140 cm^{-1})			*Rb. capsulatus* (E_a = 200 cm^{-1})		
	B_B	P	B_A	B_B	P	B_A
10 (6.9)	0	100	0	0	100	0
70 (48.6)	5	90	5	1.5	97	1.5
110 (76.3)	12	76	12	7	86	7
298 (207)	25	50	25	22	56	22

Double mutant analysis

Of interest to the interpretation of the data are the signals resulting from the double mutant strains that combine single mutants that had dramatic effects on the observed triplet signals. One such set of mutants contains RCs with the L181Phe → Lys substitution (KY, KK, and KE). The decreased transfer efficiency observed in these RCs is undoubtedly caused by the hexacoordination of B_B by L181Lys. The effect of this mutation is dominant to any effects brought about by additional substitution at M208. In a similar manner, the effect of the M208Tyr → Glu mutation, which increases transfer efficiency, appears to be dominant to the effects of the Glu substitution at L181 (compare FE, EE, and EY; Fig. 6).

In contrast, the effects of the histidine mutations appear to be additive in the double mutant HH. In the HY single mutant, transfer efficiency is decreased, but in the FH single mutant, transfer efficiency is increased. The HH double mutant shows a triplet transfer efficiency which is similar to that of the wild type; thus the effects of each single histidine substitution appear to simply cancel each other. The primary effects of the histidine substitutions are the formation of hydrogen bonds with the ring I acetyl groups of H_A and H_B (Schiffer et al., 1992; DiMagno et al., 1997), but the NE2 nitrogen atom of histidine can coordinate a water molecule and change the nature of the protein solvent in that manner. To a lesser extent, the threonine substitutions cause similar, opposite effects that cancel in the double mutant (see FT, TY versus TT; Fig. 6); we would expect that cavities that are caused by the substitution of the smaller Thr for the large aromatic Phe or Tyr would be filled by water molecules (Schiffer et al., 1995). The TTP mutant (Class II) has a transfer efficiency that appears more like that of FT (its PS^+ relative) than TT (PS^-) or TY (a PS^+ Class I mutant).

CONCLUSIONS

This study constitutes the first comprehensive report of effects of amino acid substitutions, from a family of 20 mutant strains, on the efficiency of triplet energy transfer in bacterial photosynthetic reaction centers. Triplet states were readily formed on the primary donor in the RCs of these strains because secondary electron transfer was blocked by

chemical reduction of Q_A. The observed effects of mutation of amino acids near the cofactors involved in the thermally activated Dexter process are significant, but less pronounced than effects observed with cofactor substitution. In particular, we emphasize the reduced transfer efficiency in RCs carrying a lysine at position L181, which donates a sixth ligand to the monomeric bacteriochlorophyll B_B. We postulate that hexacoordination of B_B raises its triplet energy level, and thereby disfavors electronic overlap between P and B_B, or increases the activation barrier for transfer. A hydrophobic cavity introduced by substitution of Ala for Phe at position L181 affects the rate of triplet transfer; however, a cavity introduced by substitution of a polar Thr for the same Phe does not, nor does substitution of the acidic residue, L181Glu. In contrast, are several polar substitutions at M208 that increase the observed triplet transfer efficiency at temperatures $\geq$ 70 K. Our results provide new insights into structure/function relationships in the photosynthetic reaction center. This complex is an important model for understanding protein modulation of carotenoid function at atomic resolution. In addition, this work details the involvement of the intervening bacteriochlorophyll in the energy transfer scheme and will aid in explaining the variation in transfer efficiencies that is observed in RCs isolated from different species of purple, nonsulfur bacteria.

We thank E. Bylina for the gift of the carotenoidless *Rb. capsulatus* deletion strain U43B.

The work at Argonne National Laboratory was supported by the U.S. Department of Energy (DOE), Office of Biological and Environmental Research (MS and DKH) and Office of Basic Energy Sciences, Division of Chemical Sciences (MCT), under contract no. W-31-109-ENG-38. Some of the activities were partially supported by Argonne National Laboratory Research and Development funds. MS and DKH were also supported by Public Health Service grant 5 RO1 GM36598. The work at the University of Connecticut was supported by grants from the Public Health Service (GM30353), the Human Frontier Science Program, the United States Department of Agriculture (92-37306-7690), and the University of Connecticut Research Foundation. PDL acknowledges an appointment to the Alexander Hollaender Postdoctoral Research Program sponsored by the U.S. DOE, Office of Biological and Environmental Research, and administered by the Oak Ridge Institute for Science and Education.

REFERENCES

Angerhofer, A., and V. Aust. 1993. Monomeric bacteriochlorophyll triplet state (^{3}B) in reaction centres of *Rhodobacter sphaeroides* R26, studied by absorption-detected magnetic resonance. *Photochem. Photobiol. B.* 20:127–132.

Arnoux, B., A. Ducruix, F. Reiss-Husson, M. Lutz, J. Norris, M. Schiffer, and C. H. Chang. 1989. Structure of spheroidene in the photosynthetic reaction center from Y *Rhodobacter sphaeroides. FEBS Lett.* 58:47–50.

Arnoux, B., J.-F. Gaucher, A. Ducruix, and F. Reiss-Husson. 1995. Structure of the photochemical reaction centre of a spheroidene-containing purple bacterium, *Rhodobacter sphaeroides* Y, at 3 Å resolution. *Acta Crystallogr.* D51:368–379.

Atkins, P. W. 1990. Physical Chemistry, 4th Ed. W. H. Freeman, New York.

Breton, J. 1988. Low temperature linear dichroism study of the orientation of the pigments in reduced and oxidized reaction centers of *Rps. viridis* and *Rb. sphaeroides. In* The Photosynthetic Bacterial Reaction Center. J. Breton and A. Vermeglio, editors. Plenum, New York. 59–69.

Budil, D. E., P. Gast, C. H. Chang, M. Schiffer, and J. R. Norris. 1987. Three-dimensional X-ray crystallography of membrane proteins: insights into electron transfer. *Annu. Rev. Phys. Chem.* 38:561–583.

Budil, D. E., and M. C. Thurnauer. 1991. The chlorophyll triplet state as a probe of structure and function in photosynthesis. *Biochim. Biophys. Acta.* 1057:1–41.

Bylina, E. J., S. V. Kolaczkowski, J. R. Norris, and D. C. Youvan. 1990. EPR characterization of genetically modified reaction centers of *Rhodobacter capsulatus. Biochemistry.* 29:6203–6210.

Bylina, E. J., R. V. M. Jovine, and D. C. Youvan. 1989. A genetic system for rapidly assessing herbicides that compete for the quinone binding site of photosynthetic reaction centers. *BioTechnology.* 7:69–74.

Callahan, B. M., and T. M. Cotton. 1987. Assignment of bacteriochlorophyll a ligation state from absorption and resonance Raman spectra. *J. Am. Chem. Soc.* 109:7001–7007.

Chadwick, B. W., and H. A. Frank. 1986. Electron spin resonance studies of carotenoids incorporated into reaction center of *Rhodobacter sphaeroides* R-26.1. *Biochim. Biophys. Acta.* 851:257–266.

Chang, C.-H., O. El-Kabbani, D. M. Tiede, J. R. Norris, and M. Schiffer. 1991. The structure of the membrane-bound photosynthetic reaction center from *Rhodobacter sphaeroides. Biochemistry.* 30:5352–5360.

Closs, G. L., M. D. Johnson, J. R. Miller, and P. Piotrowiak. 1989. A connection between intramolecular long-range electron, hole, and triplet energy transfers. *J. Am. Chem. Soc.* 111:3751–3753.

Cogdell, R. J., and H. A. Frank. 1987. How carotenoids function in photosynthetic bacteria. *Biochim. Biophys. Acta.* 895:63–79.

Deisenhofer, J., O. Epp, K. Miki, R. Huber, and H. Michel. 1985. Structure of the protein subunits in the photosynthetic reaction center from *Rsp. viridis* at 3 Å resolution. *Nature.* 318:618–624.

Deisenhofer, J., O. Epp, I. Sinning, and H. Michel. 1995. Crystallographic refinement at 2.3 Å resolution and refined model off the photosynthetic reaction centre from *Rhodopseudomonas viridis. J. Mol. Biol.* 246: 429–457.

Dexter, D. L. 1953. A theory of sensitized luminescence in solids. *J. Chem. Phys.* 21:836–850.

DiMagno, T. J., P. D. Laible, N. R. Reddy, G. J. Small, R. J. Norris, M. Schiffer, and D. K. Hanson. 1997. Protein-chromophore interactions: spectral shifts report the consequences of mutations in the bacterial photosynthetic reaction center. *Spectrochim. Acta A.* (in press).

El-Kabbani, O., C.-H. Chang, D. Tiede, J. Norris, and M. Schiffer. 1991. Comparison of reaction centers from *Rhodobacter sphaeroides* and *Rhodopseudomonas viridis*: overall architecture and protein-pigment interactions. *Biochemistry.* 30:5361–5369.

Ermler, U., G. Fritzsch, S. K. Buchanan, and H. Michel. 1994. Structure of the photosynthetic reaction centre from *Rhodobacter sphaeroides* at 2.65 Å resolution. *Structure.* 2:925–936.

Farhoosh, R., V. Chynwat, R. Gebhard, J. Lugtenburg, and H. A. Frank. 1994. Triplet energy transfer between bacteriochlorophyll and carotenoids in B850 light-harvesting complexes of *Rhodobacter sphaeroides* R-26.1. *Photosynth. Res.* 42:157–166.

Frank, H. A., V. Chynwat, G. Hartwich, M. Meyer, I. Katheder, and H. Scheer. 1993a. Carotenoid triplet state formation in *Rhodobacter sphaeroides* R-26 reaction centers exchanged with modified bacteriochlorophyll pigments and reconstituted with spheroidene. *Photosynth. Res.* 37:193–203.

Frank, H. A., V. Chynwat, A. Posteraro, G. Hartwich, I. Simonin, and H. Scheer. 1996. Triplet state energy transfer between the primary donor and the carotenoid in *Rhodobacter sphaeroides* R-26.1 reaction centers exchanged with modified bacteriochlorophyll pigments and reconstituted with spheroidene. *Photochem. Photobiol.* 64:823–831.

Frank, H. A., R. Friesner, J. A. Nairn, G. C. Dismukes, and K. Sauer. 1979. The orientation of the primary donor in bacterial photosynthesis. *Biochim. Biophys. Acta.* 547:484–501.

Frank, H. A., J. Innes, M. Aldema, R. Neumann, and C. Schenck. 1993b. Triplet state EPR of reaction centers from the HisL173 $\rightarrow$ LeuL173 mutant of *Rhodobacter sphaeroides* which contains a heterodimer primary donor. *Photosynth. Res.* 38:99–109.

Frick, J., J. U. von Schütz, H. C. Wolf, and G. Kothe. 1990. First detection of the (nonphosphorescent) triplet state in single crystals of β-carotene. *Mol. Cryst. Liq. Cryst.* 183:269–272.

Haberkorn, R., M. E. Michel-Beyerle, and R. A. Marcus. 1979. On spin-exchange and electron-transfer rates in bacterial photosynthesis. *Proc. Natl. Acad. Sci. USA.* 76:4185–4188.

Hartwich, G., H. Scheer, V. Aust, and A. Angerhofer. 1995. Absorption and ADMR studies on bacterial reaction centers with modified pigments. *Biochim. Biophys. Acta.* 1230:97–113.

Hoff, A. J., and I. I. Proskuryakov. 1985. Triplet EPR spectra of the primary electron donor in bacterial photosynthesis at temperatures between 15 and 296 K. *Chem. Phys. Lett.* 115:303–310.

Jia, Y., T. J. DiMagno, C-K. Chan, Z. Wang, M. Du, D. K. Hanson, M. Schiffer, J. R. Norris, G. R. Fleming, and M. S. Popov. 1993. Primary charge separation in mutant reaction centers of *Rhodobacter capsulatus*. *J. Phys. Chem.* 97:13180–13191.

Kirmaier, C., and D. Holten. 1987. Primary photochemistry of reaction centers from the photosynthetic purple bacteria. *Photosynth. Res.* 13: 225–260.

Kolaczkowski, S. V., E. J. Bylina, D. C. Youvan, and J. R. Norris. 1990. Examination of the *Rhodobacter capsulatus* special pair in wild-type and heterodimer-containing reaction centers by time-resolved optically detected magnetic resonance. *In* Molecular Biology of Membrane-Bound Complexes in Phototrophic Bacteria. G. Drews, editor. Plenum, New York. 305–312.

Krasnovsky, A. A., Jr., M. E. Bashtanov, N. N. Drozdova, P. A. Liddell, A. L. Moore, T. A. Moore, and D. Gust. 1997. Porphyrin and pyropheophorbide phosphorescence in synthetic molecules that mimic photosynthetic triplet energy transfer. *J. Photochem. Photobiol. A.* 102:157–161.

Lamola, A. A. 1969. Electronic energy transfer in solution: theory and applications. *In* Energy Transfer and Organic Photochemistry. A. A. Lamola, J. J. Turro, P. A. Leermakers, and A. Weissberger, editors. Interscience Publishers, New York. 17–132.

Lang, E., W. Lersch, P. Tappermann, W. J. Coleman, D. C. Youvan, R. Feick, and M. E. Michel-Beyerle. 1990. High power RYDMR spectra of P^+H^- in reaction centers of photosynthetic bacteria. *In* Current Research in Photosynthesis, Vol. I. M. Baltscheffsky, editor. Kluwer, Dordrecht, the Netherlands. 149–152.

Levanon, H., and J. R. Norris. 1978. The photoexcited triplet state and photosynthesis. *Chem. Rev.* 78:185–198.

McGann, W. J., and H. A. Frank. 1985. Transient electron spin resonance spectroscopy of the carotenoid triplet state in *Rhodopseudomonas sphaeroides* wild type. *Chem. Phys. Lett.* 121:253–261.

Moser, C. C., J. M. Keske, D. Warncke, R. S. Farid, and P. L. Dutton. 1992. Nature of biological electron transfer. *Nature.* 355:796–802.

Norris, J. R., D. E. Budil, M. K. Bowman, J. Tang, C. A. Wraight, and G. L. Closs. 1982. Magnetic characterization of the primary state of bacterial photosynthesis. *Proc. Natl. Acad. Sci. USA.* 79:5532–5536.

Norris, J. R., D. E. Budil, P. Gast, C.-H. Chang, O. El-Kabbani, and M. Schiffer. 1989. Correlation of paramagnetic states and molecular structure in bacterial photosynthetic reaction centers: the symmetry of the primary electron donor in *Rhodopseudomonas viridis* and *Rhodobacter sphaeroides* R-26. *Proc. Natl. Acad. Sci. USA.* 86:4335–4339.

Norris, J. R., and M. C. Thurnauer. 1978. Magnetic resonance spectroscopy of the primary donor of photosynthesis. *In* Proceedings of the Third International Seminar on Energy Transfer in Condensed Matter, Univerzita Karlova Praha, Prague. J. Fiala, editor. 72.

Popov, M. 1996. Effects of point mutations on the energetics of the photosynthetic reaction centers. Thesis. University of Chicago, Chicago, IL.

Prince, R., and D. C. Youvan. 1987. Isolation and spectroscopic properties of photochemical reaction centers from *Rhodobacter capsulatus*. *Biochim. Biophys. Acta.* 890:286–291.

Schenck, C. C., R. E. Blankenship, and W. W. Parson. 1982. Radical-pair decay kinetics, triplet yields and delayed fluorescence from bacterial reaction centers. *Biochim. Biophys. Acta.* 680:44–59.

Schenck, C. C., P. Mathis, and M. Lutz. 1984. Triplet formation and triplet decay in reaction centers from the photosynthetic bacterium *Rhodopseudomonas sphaeroides*. *Photochem. Photobiol.* 39:407–417.

Schiffer, M., C. F. Ainsworth, Y.-L. Deng, G. Johnson, F. H. Pascoe, and D. K. Hanson. 1995. Proline in a transmembrane helix compensates for cavities in the photosynthetic reaction center. *J. Mol. Biol.* 252:472–482.

Schiffer, M., C.-K. Chan, C.-H. Chang, T. J. DiMagno, G. R. Fleming, S. L. Nance, J. R. Norris, S. Snyder, M. C. Thurnauer, D. M. Tiede, and D. K. Hanson. 1992. Study of reaction center function by analysis of the effects of site-specific and compensatory mutations. *In* The Photosynthetic Bacterial Reaction Center II, NATO ASI Series. J. Breton and A. Vermeglio, editors. Plenum, London. 251–261.

Shuvalov, V. A., and W. W. Parson. 1981. Energies and kinetics of radical pairs involving bacteriochlorophyll and bacteriopheophytin in bacterial reaction centers. *Proc. Natl. Acad. Sci. USA.* 78:957–961.

Simon, R., U. Priefer, and A. Puhler. 1983. A broad host range mobilization system for in vivo genetic engineering: transposon mutagenesis in Gram negative bacteria. *BioTechnology.* 1:37–45.

Stowell, M. H. B., T. M. McPhillips, D. C. Rees, S. M. Soltis, E. Abresch, and G. Feher. 1997. Light-induced structural changes in photosynthetic reaction center: implications for mechanism of electron-proton transfer. *Science.* 276:812–816.

Takiff, L., and S. G. Boxer. 1988a. Phosphorescence from the primary electron donor in *Rhodobacter sphaeroides* and *Rhodopseudomonas viridis* reaction centers. *Biochim. Biophys. Acta.* 932:325–334.

Takiff, L., and S. G. Boxer. 1988b. Phosphorescence spectra of bacteriochlorophylls. *J. Am. Chem. Soc.* 110:4425–4426.

Thurnauer, M. C. 1979. ESR study of the photoexcited triplet state in photosynthetic bacteria. *Rev. Chem. Int.* 1:197–230.

Thurnauer, M. C., J. J. Katz, and J. R. Norris. 1975. The triplet state in bacterial photosynthesis: possible mechanisms of the primary photo-act. *Proc. Natl. Acad. Sci. USA.* 72:3270–3274.

Thurnauer, M. C., and J. R. Norris. 1976. Magnetophotoselection applied to the triplet state observed by EPR in photosynthetic bacteria. *Biochem. Biophys. Res. Commun.* 73:501–506.

Xiao, W., S. Lin, A. K. W. Taguchi, and N. W. Woodbury. 1994. Femtosecond pump-probe analysis of energy and electron transfer in photosynthetic membranes of *Rhodobacter capsulatus*. *Biochemistry.* 33: 8313–8322.

Yeates, T. O., H. Komiya, A. Chirino, D. C. Rees, J. P. Allen, and G. Feher. 1988. Structure of the reaction center from *Rhodobacter sphaeroides* R-26 and 2.4.1: protein-cofactor (bacteriochlorophyll, bacteriopheophytin, and carotenoid) interactions. *Proc. Natl. Acad. Sci. USA.* 85:7993–7997.

Youvan, D. C., S. Ismail, and E. J. Bylina. 1985. Chromosomal deletion and plasmid complementation of the photosynthetic reaction center and light-harvesting genes from *Rhodopseudomonas capsulata*. *Gene.* 33: 19–30.